Journal of Marine Science and Application (2024) 23: 947-959
https://doi.org/10.1007/s11804-024-00471-w

RESEARCH ARTICLE

Robust Path Following Control of AUVs Using Adaptive Super Twisting SOSMC

Raghavendra M. Shet[1], Girish V. Lakhekar[2], Nalini C. Iyer[1] and Laxman M. Waghmare[3]

Received: 23 November 2023 / Accepted: 27 March 2024

Abstract

The path-following control design for an autonomous underwater vehicle (AUV) requires prior full or partial knowledge about the mathematical model defined through Newton's second law based on a geometrical investigation. AUV dynamics are highly nonlinear and time-varying, facing unpredictable disturbances due to AUVs operating in deep, hazardous oceanic environments. Consequently, navigation guidance and control systems for AUVs must learn and adapt to the time-varying dynamics of the nonlinear fully coupled vehicle model in the presence of highly unstructured underwater operating conditions. Many control engineers focus on the application of robust model-free adaptive control techniques in AUV maneuvers. Hence, the main goal is to design a novel salp swarm optimization of super twisting algorithm-based second-order sliding mode controller for the planar path-following control of an AUV through regulation of the heading angle parameter. The finite time for tracking error convergence in the horizontal plane is provided through the control structure architecture, particularly for lateral deviations from the desired path. The proposed control law is designed such that it steers a robotic vehicle to track a predefined planar path at a constant speed determined by an end-user, without any temporal specification. Finally, the efficacy and tracking accuracy are evaluated through comparative analysis based on simulation and experimental hardware-in-loop assessment without violating the input constraints. Moreover, the proposed control law can handle parametric uncertainties and unpredictable disturbances such as ocean currents, wind, and measurement noise.

Keywords Autonomous underwater vehicle; Super twisting second-order sliding mode control; Salp Swarm optimization; Planar path following control and hardware-in-loop

1 Introduction

The ocean is a rich source of energy and plays a key role in forecasting variations in the earth's climate. Hence, numerous studies have been performed to explore natural resources and assist with underwater robotic manipulators and vehicles. Autonomous underwater vehicles (AUVs) are generally employed in underwater interventions owing to their excellent maneuvering capabilities and high accuracy in path-following control in spatial space (Guo et al., 2003). Studies on underwater robotic vehicles have increased over the past two to three decades. Owing to improvements in technology and the capacity to create intelligent, smarter robots, autonomous vehicles are employed for more expeditions. This situation enables exploring higher-risk areas, spending more time underwater, and conducting more productive underwater applications compared with human-piloted/tethered underwater vehicles (Fossen, 1994). These vehicles have been engineered to be strong, adaptable, and agile. Consequently, during the past 25 years, substantial research has been devoted to developing AUVs that can perform a wide range of tasks that are much beyond the scope of divers and small submarines; the tasks include long-term sample collection and 3D mapping of underwater tunnels. These vehicles can dive deeper and stay submerged for longer periods of time without risking people (Lakhekar and Waghmare, 2014).

Controlling underwater vehicles is very challenging due to nonlinear, time-varying, and unexpected external disturbances, including sea current fluctuations, which oppose

Article Highlights

- An adaptive super-twisting algorithm-based second-order sliding mode control scheme is designed for the stabilization and path-following control of the nonlinear autonomous underwater vehicle (AUV) model.
- An appropriate adaptive parameter-tuning law is proposed for hitting gain and sliding surface slope through the salp swarm optimization algorithm to dominate the perturbations of the system without the information of their upper bounds.
- A path-following control algorithm is presented to establish a chattering-free robust performance and finite-time convergence for the AUV model.
- The effectiveness of the proposed technique is validated by demonstrative simulation results and experimental assessments.

✉ Raghavendra M. Shet
raghu@kletech.ac.in

[1] School of Electronics and Communication, KLE Technological University, Hubballi 580031, Karnataka, India

[2] Department of Instrumentation and Control Engineering, COEP Technological University, Pune 411005, Maharashtra, India

[3] Central University of Rajasthan, Bandarsindhri 305817, Krishnagar, Ajmer, India

the motion of AUVs. Because the dynamics of an AUV are inherently complicated, nonlinear, and time-varying, it can neither be neglected nor considerably simplified while designing controls. Additionally, depending on the operating circumstances, its mass and buoyancy changes (Elmokadem et al., 2016). The difficulty in precisely simulating the hydrodynamic effect and Coriolis force is a substantial impediment to AUV autonomy. AUV actuators can generate a limited amount of torque. During AUV operation, torque requirements may surpass the AUV's torque limit. Thus, actuator saturation is inevitable. This outcome demonstrates that actuator saturation is a substantial issue in the motion control of AUVs. Because linear controllers function locally in water, where manually tweaking the control settings is challenging, linear controllers may not satisfy the desired requirements, specifically when operating conditions or the system environment change (Sahu and Subudhi, 2014). Despite remarkable progress in the field of control design strategies that enable the vehicle to operate under parametric uncertainty, varying dynamics, unbounded constraints and failures, still need to be developed (Rout and Subudhi, 2016). Two aspects contribute to the challenges in the field of marine robotics: First, the complex dynamics of marine vehicles cannot be disregarded or dramatically minimized during the design of the control scheme. Second, the designed control scheme is dependent on unmeasured states. AUVs pose a control challenge because a majority of them are underactuated, imposing nonintegrable acceleration constraints (Lakhekar and Roy, 2014) by having fewer actuated inputs than degrees of freedom (DOF). To address this issue, researchers have developed advanced control approaches that include intelligence, adaptive capacity, rapid convergence, and resilience (Lakhekar and Saundarmal, 2013). Nevertheless, throughout the last several decades, much attention has been devoted to developing a variety of acceptable control approaches for underwater vehicle motion control in ocean engineering (Nakamura and Savant, 1992). These approaches include traditional PD/PID control (Jalving, 1994), sliding mode control (SMC; Yoerger and Slotine, 1985), quasi-SMC (Shet et al., 2023), self-adjusting control (Goheen and Jefferys, 1990), suboptimal control (Geranmehr and Nekoo, 2015), LQG control (Naeem et al., 2003), gain scheduling-based control (Silvestre et al., 2002), feedback control (Pisano and Usai, 2004), backstepping method (Rout and Subudhi, 2016), linear matrix inequality (LMI) convex approach (Innocenti and Campa, 1999), $H\infty$ control (Feng and Allen, 2004), and Riccati equation-based control (Naik and Singh, 2007). Here, most controllers were developed with no or very minimal knowledge of hydrodynamic coefficients and maritime instabilities such as waves and currents (Antonelli et al., 2001). Intelligent methods used for control, such as neural networks (NN) (Yuh, 1990), fuzzy logic control (FLC) (DeBitetto, 1995), genetic algorithms (GA) (Moura et al., 2010), self-organizing control (Lakhekar and Waghmare, 2023), and adaptive neuro-fuzzy control (Lakhekar et al., 2020), offer a more practical solution for route tracking control in such situations.

By contrast, well-documented disadvantages of intelligent control include the following: Conventional FLC requires specialist knowledge about vehicle operating conditions and several trial-and-error cycles. Suppose the controlled plant is unpredictable and nonlinear, FLC with fixed scaling factors and tedious rules may fail (Lakhekar and Roy, 2014). While training time is uncertain in the case of NN-based control, it may not be acceptable for practical application. Furthermore, NN has the drawback of requiring a lengthy training period and a sluggish pace, so many systems are incapable of handling it. In addition, NNs fail to meet essential characteristics such as quick response and minimum computation overload (Yuh, 1990). While GA-based control schemes cannot ensure their stability, they are frequently utilized as compensatory in most previous research works (Moura et al., 2010). Nonlinearities in the system are not considered by linear quadratic regulators and LQG, which may lead to poor performance and even instability in maneuvering operations (Naeem et al., 2003). Adaptive control appears more effective for handling model uncertainty (Antonelli et al., 2001), but it requires a large amount of computer power for multivariable higher-order nonlinear systems. Of these, the SMC robust control scheme provides a decent path-tracking performance with an easy-to-understand layout, but it has undesired high control activity in the steady-state zone. To compensate for the effect of chattering and the unmodeled dynamics of the vehicle, researchers have revised and extended the robust sliding mode technique to adaptive terminal SMC (Lakhekar and Waghmare 2018). The integral SMC technique is also used to reject and overcome the effects of unpredictable disturbance due to ocean waves, tides, and currents to stabilize an AUV in ocean space (Kim et al., 2015). The second-order sliding mode control (SOSMC) technique requires the upper bound of uncertainty, which is challenging to determine accurately in advance for practical applications. The reduction of the chattering effect is remarkably influenced by the most suitable choice of hitting gain, which is facilitated by salp swarm optimization (SSWO) (Cheng and Wang, 2020). With fast vehicle convergence to the predetermined planar path, the super twisting algorithm (STA) proposed in this paper aims to overcome the flaws and improve the SOSMC approach. STA – SMC creates a smooth, continuous control signal, thus resolving the chattering issue and achieving high accuracy under the effect of quick disturbances (Chalanga et al., 2016).

The main contributions of this paper compared with the related investigations are listed as follows:

• An adaptive STA-based second-order SMC scheme is designed for the stabilization and path-following control of the nonlinear AUV model.

• An appropriate adaptive parameter-tuning law is suggested for hitting gain and sliding surface slope through the SSWO algorithm to dominate the perturbations of the system without the information of their upper bounds.

• A path-following control algorithm is proposed to establish a chatter-free robust performance and finite-time convergence for the AUV model.

• The effectiveness of the proposed technique is verified by demonstrative simulation results and experimental assessments.

This paper is organized as follows: In Section 2, the AUV model is expressed in nonlinear form. In Section 3, the proposed overall control method is described, and optimization is explored. In Sections 4 and 5, various simulation studies and experimental hardware-in-the-loop (HIL) validation demonstrate the efficacy of the recommended efficient control technique, respectively. In Section 6, a conclusion is drawn.

2 Mathematical modeling of vehicle

Directing an AUV along a defined path at a constant forward speed is formulated in this section by discussing the kinematic and dynamic models of an AUV in the horizontal plane.

2.1 Controlled path following in a horizontal plane

The path tracking or following problem is described in X-Y plane through inertial reference frame $\{I\}$, Serret-Frenet (S-F) frame $\{F\}$, and body-fixed frame $\{B\}$, as illustrated in Figure 1. The center of mass (CM) of the AUV, is well defined along the vehicle's principal axes (such as x longitudinal axis and y transverse axis in the inertial reference frame or along axes (x_e, y_e) in the S-F frame), serves as the origin of the body-fixed frame. U is the AUV's net velocity, $U = \sqrt{u^2 + v^2}$. The line l indicates the distance between the origin of the global coordinate system $\{I\}$ and the origin of the body coordinate system $\{B\}$, k represents the distance between the origin of the global coordinate system $\{I\}$ and point S as a reference point the on S-F frame.

The AUV heading angle is denoted by ψ, the drift angle $\beta = \tan^{-1}\left(\frac{u}{v}\right)$ is expressed as the angle between the net and sway velocities in the $\{B\}$ coordinate system; the angle formed by the S-F frame and the inertial frame is denoted as θ_s. Considering a desired path Ω is followed by an AUV with its body frame attached to its center of gravity and c_c is expected curvature at point S with their length of arc s* in horizontal plane. The undersea vehicle's velocities as indicated in $\{I\}$ and $\{B\}$ are u for forward motion, v for transverse motion, and r for heading angular motion. The surge motion equation along the x-direction, the sway motion equation along the y-direction, and the yaw motion equation, which is rotational movement along the z-direction for the route following control in the x-y domain, comprise the vehicle model.

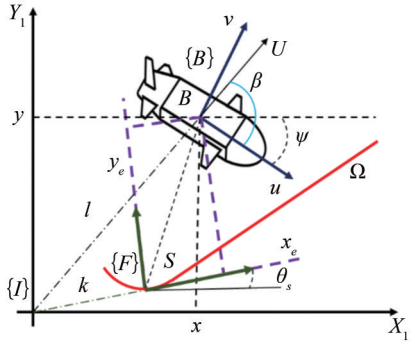

Figure 1 Serret-frenet frame parameters: Path tracking

A vehicle model's corresponding kinematic equations must also be considered. The INFANTE AUV model described in (Lapierre and Soetanto, 2007) is the basis for the model presented in this paper, and the reader is referred to it for more information. The kinematic and dynamic equations of AUV can be stated as follows.

2.2 Kinematics of AUV

An underactuated AUV's kinematic equations can be represented by rotating motion along the z-axis as well as linear motion along the x, and y axes.

$$\dot{x} = u\cos(\psi) - v\sin(\psi) \tag{1}$$

$$\dot{y} = u\sin(\psi) + v\cos(\psi) \tag{2}$$

$$\dot{\psi} = r \tag{3}$$

where (x, y) represents an AUV's linear coordinates in a fixed frame on the ground, ψ is the vehicle's yaw angle, u is the surge, v is the sway and r is the yaw velocity along the x, y, and z axes, respectively.

2.3 Dynamics of AUV

The elements that contribute to motion along the z-axis, i.e., pitch and heave motion equations, are neglected because of the motion of the AUV in the x-y plane. because the AUV in this paper is of the flat-fish variety, the roll equation of motion is ignored. The following motion equations are used as follows.

Surges equation of motion:

$$\dot{u} = \frac{m_{22}}{m_{11}} vr - \frac{X_u}{m_{11}} u - \frac{X_{u|u|}}{m_{11}} u|u| + \frac{1}{m_{11}} F_u + \frac{\tau_{Eu}}{m_{11}} \quad (4)$$

Sway equation of motion:

$$\dot{v} = -\frac{m_{22}}{m_{22}} ur - \frac{Y_v}{m_{22}} v - \frac{Y_{v|v|}}{m_{22}} v|v| + \frac{1}{m_{22}} F_v + \frac{\tau_{Ev}}{m_{22}} \quad (5)$$

Yaw equation of motion:

$$\dot{r} = \frac{m_{11} - m_{22}}{m_{33}} uv - \frac{N_r}{m_{33}} v - \frac{N_{r|r|}}{m_{33}} r|r| + \frac{\tau_{Er}}{m_{33}} \quad (6)$$

where, F_u and F_v represent the control forces of vehicle's surge and sway motions, respectively. Yaw motion equation is unregulated in vehicle dynamics, hence the AUV is reported as a dynamic model that is underactuated. The extra mass terms such as ($X_{\dot{u}}$, $Y_{\dot{v}}$) and total rigid body mass m of the vehicle comprise the parameters $m_{11} = m - X_{\dot{u}}$ and $m_{22} = m - Y_{\dot{v}}$, respectively. The collective rigid body mass of m and the additional moment of inertia about the z_b axis, denoted as $N_{\dot{r}}$, are other constants, and their values are expressed as $m_{22} = m - N_{\dot{r}}$. The coefficients of linear and quadratic drag are X_u, $X_{u|u|}$, Y_v, $Y_{v|v|}$ and N_r. Unknown environmental disturbances affecting the AUV include τ_{Ev} and τ_{Er}. To guarantee the trajectory tracking in a horizontal plane x-y plane, a 3-DOF model with input force vector is established as $\boldsymbol{\tau} = [F_u, F_v, 0]^{\mathrm{T}}$, while its velocity and attitude vector remain $\boldsymbol{v} = [u, v, r]^{\mathrm{T}}$ and $\boldsymbol{\eta} = [x, y, \psi]^{\mathrm{T}}$, respectively

$$\begin{bmatrix} m - X_{\dot{u}} & 0 & 0 \\ 0 & m - Y_{\dot{v}} & 0 \\ 0 & 0 & I_{zz} - N_{\dot{r}} \end{bmatrix} \begin{bmatrix} \dot{u} \\ \dot{v} \\ \dot{r} \end{bmatrix} + \begin{bmatrix} -X_u - X_{u|u|}|u| & 0 & 0 \\ 0 & -Y_v - Y_{v|v|}|v| & 0 \\ 0 & 0 & -N_r - N_{r|r|}|r| \end{bmatrix} \begin{bmatrix} u \\ v \\ r \end{bmatrix} + \begin{bmatrix} 0 & 0 & \left(-m + Y_{\dot{v}}\right)v \\ 0 & 0 & \left(m - X_{\dot{u}}\right)u \\ \left(m - Y_{\dot{v}}\right)v & \left(-m + X_{\dot{u}}\right)u & 0 \end{bmatrix} \begin{bmatrix} u \\ v \\ r \end{bmatrix} = \begin{bmatrix} F_u \\ F_v \\ 0 \end{bmatrix} \quad (7)$$

Generalized mathematical model of AUV is represented in standard form as follows:

$$\boldsymbol{M}(v)\dot{v} + \boldsymbol{C}(v)v + \boldsymbol{D}(v)v + \boldsymbol{g}(\eta) = \boldsymbol{\tau} \quad (8)$$

where, $\boldsymbol{M}(v)$ is inertial matrix including the added mass, $\boldsymbol{C}(v)$ is the Coriolis matrix, $\boldsymbol{D}(v)$ is the damping matrix, $\boldsymbol{g}(\eta)$ is the vector of gravitational/buoyancy forces, and moment $\boldsymbol{\tau}$ is the vector of control inputs.

2.4 Serret-frenet frame

In general, the parameters in the Serret-Frenet (S-F) frame are used to investigate the path following control problem of underactuated AUVs. Incorporating the global coordinate transformation and S-F frame, the convergence problem of the vehicle is transformed into the actuation system control problem, simplifying the controller design. The established reference path functions as the foundation for the LOS guidance, which is built in a moving S-F frame along the virtual target on the path with tangential velocity. Independent of movements, the S-F formulas convey the kinematic characteristics of a particle on a differentiable path in three dimensions. The formulas that describe the position and orientation error dynamics (route following error space model) more clearly show the derivatives of the tangent, binormal unit vectors, and normal.

2.5 Path tracking error

Using the coordinate transformation provided, a path following/tracking error dynamic model (Guo et al., 2003) is developed to simplify the construction of the controller. To follow the reference trajectory, a desired heading angle must be determined for the vehicle and is as follows

$$\psi_d = \arctan\left(\frac{\dot{y}_{\mathrm{d}}}{\dot{x}_{\mathrm{d}}}\right) \quad (9)$$

where, in an earth-fixed frame, x, y, and ψ_{d} denote the intended positions and orientations for the vehicle. The definition of the orientation error is

$$\psi_{\mathrm{e}} = \psi - \psi_{\mathrm{d}} \quad (10)$$

Its differentiation is represented as follows:

$$\dot{\psi}_{\mathrm{e}} = r - c_{\mathrm{c}}\dot{s}^* \quad (11)$$

Orientation error between total velocity U and $\dot{s}^*$ is expressed below,

$$\psi_{\mathrm{e}}^* = \psi_{\mathrm{e}} + \beta \quad (12)$$

When used with the AUV model, the orientation tracking error and positional variables derivatives are shown below,

$$\dot{x}_{\mathrm{e}} = U\cos\left(\psi_{\mathrm{e}}^*\right) - \dot{s}^*(1 - c_{\mathrm{c}}y_{\mathrm{e}}) \quad (13)$$

$$\dot{y}_{\mathrm{e}} = U\sin\left(\psi_{\mathrm{e}}^*\right) - \dot{s}^* c_{\mathrm{c}} x_{\mathrm{e}} \quad (14)$$

$$\psi_e^* = r - c_c \dot{s}^* + \dot{\beta} \tag{15}$$

2.6 Problem formulation

An underatuated AUV, represented by point B travling along the desired path Ω, which is continuously parameterized by the variable S, which in the S-F coordinate system is known as a virtual reference guidance point. The position of the variable S and the elevation angle of the point are denoted by (x_d, y_d, ψ_d). In addition, the derivatives of the reference velocity (u_d, v_d, r_d) with respect to time are constrained.

The AUV center of mass specified by (x, y, ψ) is represented by point B, which is necessary for them to converge and track the predetermined reference path. The positional error between the point S in frame $\{F\}$ and AUV is denoted by the variables x_e and y_e. The longitudinal force F_u, sway force F_v, and changing rate position are all sought after by the AUV. The tracking errors x_e and y_e become zero as the longitudinal speed u converges to the goal speed u_d.

$$\lim_{t \to \infty} x_e = 0 \tag{16a}$$

$$\lim_{t \to \infty} y_e = 0 \tag{16b}$$

$$\lim_{t \to \infty} (u - u_d) = 0 \tag{16c}$$

For position tracking errors (x_e, y_e) to converge by stabilizing u_e and v_e, the desired surge and sway velocity depends on the data of (x_d, y_d) and (x_e, y_e). Also satisfies the following condition proposed in (Rout and Subudhi, 2016)

$$u_d = \cos(\psi)\dot{x}_d + \sin(\psi)\dot{y}_d - k_1\left(\cos(\psi)x_e + \sin(\psi)y_e\right) \tag{17a}$$

$$v_d = -\sin(\psi)\dot{x}_d + \cos(\psi)\dot{y}_d + k_2\left(\sin(\psi)x_e - \cos(\psi)y_e\right) \tag{17b}$$

where the positive constant parameters k_1 and k_2 are present. The desired position tracking errors and planar path determine the required surge velocity and sway velocity. The derivative of (u_d, v_d) is calculated as shown below,

$$\dot{u}_d = \cos(\psi)\ddot{x}_d + \sin(\psi)\ddot{y}_d + v_{dr} - k_1\left(\cos(\psi)\dot{x}_e + \sin(\psi)\dot{y}_e\right) \tag{18a}$$

$$\dot{v}_d = -\sin(\psi)\ddot{x}_d + \cos(\psi)\ddot{y}_d - u_{dr} + k_2\left(\sin(\psi)\dot{x}_e - \cos(\psi)\dot{y}_e\right) \tag{18b}$$

These variables are considered during the design of control for AUV's guidance system for path-planning algorithm to minimize tracking errors and prevent issues in real-world applications.

Remark 1: Because the nonzero reference surge velocity is positive or negative, the condition $|u_{d(t)}| \geqslant u_{dmin}, \forall t \geqslant 0$, incorporates path tracking in forward and backward directions. In fact, the persistently exciting condition on the yaw reference velocity is substantially more restricted than the condition $|u_{d(t)}| \geqslant u_{dmin}, \forall t \geqslant 0$. Because of high resisting force and lack of control input during motion in the yaw axis for AUVs, the condition $|v_{d(t)}| < |u_{d(t)}|, \forall t \geqslant 0$ means the AUV system cannot track a large spiral curvature with twist.

Assumption 1. (i) The center of buoyancy (CB) and center of mass (CM) are congruent. (ii) The mass distribution of vehicle body is uniform. (iii) Heave, pitch, and roll motions, as well as terms higher than second order hydrodynamic drag, are disregarded.

Assumption 2. The reference signals u_d, v_d, and r_d are bounded. u_{dmin} is strictly positive constant, such that $|u_{d(t)}| \geqslant u_{dmin}, \forall t \geqslant 0$. The sway velocity satisfies $|v_{d(t)}| < |u_{d(t)}|, \forall t \geqslant 0$.

Assumption 3. The undiscovered environmental disturbances are constrained, namely, $|\tau_{Eu}| \leqslant \tau_{Eumax}$, $|\tau_{Ev}| \leqslant \tau_{Evmax}$, and $|\tau_{Er}| \leqslant \tau_{Ermax}$. where, τ_{Eumax}, τ_{Evmax}, and τ_{Ermax} are constants and $|.|$ indicates a variable's absolute value.

Assumption 4. The AUV system's unmodeled dynamics are constrained. Positive constants ε_u, ε_v, and ε_r are positive constants such that $\overline{\varepsilon_u}$, $\overline{\varepsilon_v}$, and $\overline{\varepsilon_r}$ satisfy the relationships $|\varepsilon_u| \leqslant \varepsilon_u$, $|\varepsilon_v| \leqslant \varepsilon_v$ and $|\varepsilon_r| \leqslant \varepsilon_r$.

3 Controller design

The two sections of the derivation of the suggested control method for an AUV's steering motion are 2-SMC and Salp swarm optimization. The following subsections descript each control part.

3.1 Second-order sliding mode control (SOSMC)

First, sliding manifold σ based on tracking error is defined as follows:

$$\sigma = \left(\Lambda + \frac{\mathrm{d}}{\mathrm{d}t}\right)^{n-1} e_c \tag{19}$$

where $e_c = \eta_c - \eta$ is the velocity error between the underwater vehicle's actual velocity and the virtual velocity created by the velocity controller, σ is the first order sliding manifold. The order of the uncontrolled system is n, and Λ is a positive constant. Raising the order of the sliding mode manifold, SOSMC achieves zero steady-state error and eliminates chattering by adding the integral term to a first-order sliding manifold. The resulting second order sliding surface is given as follows:

$$\dot{\sigma} + \zeta\sigma = \dot{e_c} + 2\Lambda e_c + \Lambda^2 \int e_c \, dt \tag{20}$$

where ζ determines the rate of decay for switching surface. The derivative of the given sliding manifold is taken, and then the scond-order manifold is obtained as follows:

$$\ddot{\sigma} + \zeta\dot{\sigma} = \left(\ddot{\eta}_c - \ddot{\eta}\right) + 2\Lambda\dot{e}_c + \Lambda^2 e_c = 0 \tag{21}$$

The general form of AUV modelling equation is substituted as follows:

$$\left(\ddot{\eta}_c - \frac{1}{M(\eta)}\left(\tau_\eta - C(v) - D(v) - g(\eta)\right)\right) + 2\Lambda\dot{e}_c + \Lambda^2 e_c = 0 \tag{22}$$

An equivalent control regulation can be derived as follows:

$$\tau_{eq} = \hat{M}\left(\ddot{\eta}_c + 2\Lambda\dot{e}_c + \Lambda^2 e_c\right) + \hat{C}(v) + \hat{D}(v) + \hat{g}(\eta) \tag{23}$$

where, $\hat{M}$, $\hat{C}$, $\hat{D}$ and $\hat{g}$ are estimated terms of AUV model. To address the resulting chattering issue, an adaptive term is included in the control rule to replace the switching term,

$$\tau_{ad} = \hat{\tau}_{test} + \left(K + \frac{\hat{C}(v)}{2\Lambda}\right)\sigma \tag{24}$$

where $\hat{\tau}_{test}$ is an adaptive term that estimates the lumped uncertainty vector as an unknown dynamic of vehicle. The estimation of the lumped uncertainty vector is approximated as (Wang et al., 2023a)

$$\dot{\hat{\tau}}_{test} = \Gamma\sigma \tag{25}$$

The overall control law can be defined along with super twisting algorithm as a disturbance observer as follows:

$$\tau_n = \tau_{eq} + \tau_{ad} + \tau_{STA} = \tau_{eq} + \hat{\tau}_{test} + \left(K + \frac{\hat{C}(v)}{2\Lambda}\right)\sigma + \left(-\mu_0 \int_0^t \mathrm{sgn}(\sigma)\, dt - \mu_1 |\sigma|^{0.5} \mathrm{sgn}(\sigma)\right) \tag{26}$$

Control inputs $\boldsymbol{\tau}_n = [F_u, F_v]$ are then applied to the dynamic model of the vehicle to produce the actual surge and lateral velocity in the body fixed frame in the horizontal plane. To solve the chattering issue in conventional SMC and to reduce the influence of quick acting disturbances, STA technique is utilized to generate a smooth and continuous control signal (Chalanga et al., 2016; Kumar et al., 2022; Sadala and Patre, 2020). The STA technique presented in for steady tracking performance uses the control gains μ_0 and μ_1, which are positive constants. The adaptive term included in control part to reduces the effect of parametric variations in sea environment. Salp Swarm optimization is used to search for best fit for K and Λ for reducing magnitude of chattering and speed of response.

3.2 Salp swarm optimization

Cheng and Wang (2020), Wang et al. (2023a), and Wang et al. (2023b) discussed the SSWO bioinspired optimization technique. Salp belongs to the family of Salpidae, which moves like jellyfish by pumping water to move forward, as shown in Figure 2.

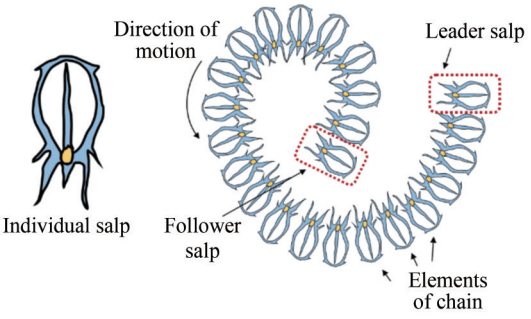

Figure 2 Social structure of swarm of salp (Salp chain)

The salp population has two mathematical groups, namely, the leader, and followers. The leader or head salp directs the salp chain and the swarm in deep water areas, whereas the rest of the salps are considered as followers. Their main objective is to investigate the food source A in the search area. The location of the leader is altered in relation to the food source, which causes the position of the following salp to shift. The position of the food supply is changed frequently in SSWO. Even if the population declines, the salp chain can pursue the food supply in the best way possible. Another benefit is the presence of only one regulating parameter, and the leading salp position is frequently updated in relation to the food source. As the search space is explored and search space exploitation starts, the number of iterations gradually decreases. This method is preferable to the current optimal algorithm because it avoids local solutions to the problem. The social structure of the salp swarm is shown in Figure 2.

The position of salps is defined in swarm-based algorithms in an m-dimensional search space, where m is the number of variables in a particular problem. As a result, a two-dimensional matrix is used to hold the positions of all salps. Presumably, the swarm uses food source A as its goal in the search space. Using the formula below, the leader's position is updated,

$$x_j^1 = \begin{cases} A_j + c_1\left(\left(u_j - l_j\right)c_2 + l_j\right), & \text{for } c_3 \geqslant 0 \\ A_j - c_1\left(\left(u_j - l_j\right)c_2 + l_j\right), & \text{for } c_3 < 0 \end{cases} \tag{27}$$

where, x_j^1 represents the position of the salp (leader) in the j^{th} dimension, A_j represents the location of the food supply in the j^{th} dimension, u_j, l_j represent the upper, lower bounds of the j_0^{th} dimension, respectively, c_1, c_2, c_3 represent random numbers.

An objective function is used to determine best fit appropriate values of control parameters, such as hitting gain K and sliding surface slope Λ. The cost function is defined such that the selected parameters minimize the error to reduce chattering simultaneously. The cost function is defined as follows

$$J_c = \int \left[W_1\left(\sigma^2\right) + W_2\left(e_k{}^2\right) \right] \mathrm{d}t \tag{28}$$

where, e_k is the tracking error function, and W_1 and W_2 are the weighting fators used in optimization technique. According to the cost function, the leader adjusts its position in relation to the food supply. The most crucial SSWO parameter is the coefficient c_1, which balances the specified exploration and exploitation.

$$c_1 = 2\mathrm{e}_k^{\left(\frac{4l}{L}\right)^2} \tag{29}$$

where, L represents maximum number of iterations, l represents current iteration. Random numbers in the range [0, 1] are generated evenly for the parameters c_2 and c_3. They specify the step size and whether the succeeding point in j^{th} dimension should point in either direction of infinity. Newton's law of motion is applied to the following equation to update the position of the followers.

$$x_j^i = \frac{1}{2}at^2 + b_0 t \tag{30}$$

where, b_0 represents initial speed, t is the time, $i \geqslant 2, x_j^i$ depicts the location of i^{th} follower salp in j^{th} dimension, and $a = \frac{b_{\text{final}}}{b_0}$ and $b = \frac{x - x_0}{t}$. Because the time for optimization is iteration, the discrepancy between iterations equals 1, and considering $b_0 = 0$, the position of follower can be expressed as follows:

$$x_j^i = \frac{1}{2}\left(x_j^i + x_j^{i-1}\right) \tag{31}$$

where, $i \geqslant 2, x_j^i$ provides the position of i^{th} follower salp in j^{th} dimension. Thanks to Wang, et al., (2023a); Wang, et al., (2023b), simulating the salp chains is possible. The advantages of the SSWO algorithm come from its ability to improve the initial random solutions efficiently and converge to the best result. The adaptive behavior of this algorithm, which makes it superior to other algorithms, is the major cause of SSWO excellence. SSWO outperforms other swarm-based strategies because it engages in more exploration during optimizion. Moreover, SSWO strongly encourages the use of the c_1 parameter in the latter stages of optimization. As a result, SSWO performs better in terms of outcome accuracy than evolutionary algorithms. The flowchart for SSWO is shown in Figure 3.

This method not only improves the search intensity of salp swarm algorithm but also increases its diversity. The optimization algorithm ensures that the algorithm can find the optimal value of the algorithm and avoid falling into the local optimum, and the algorithm has better global search capabilities due to its enhanced diversity. The optimization effect of hitting gain and sliding surface slope can be improved.

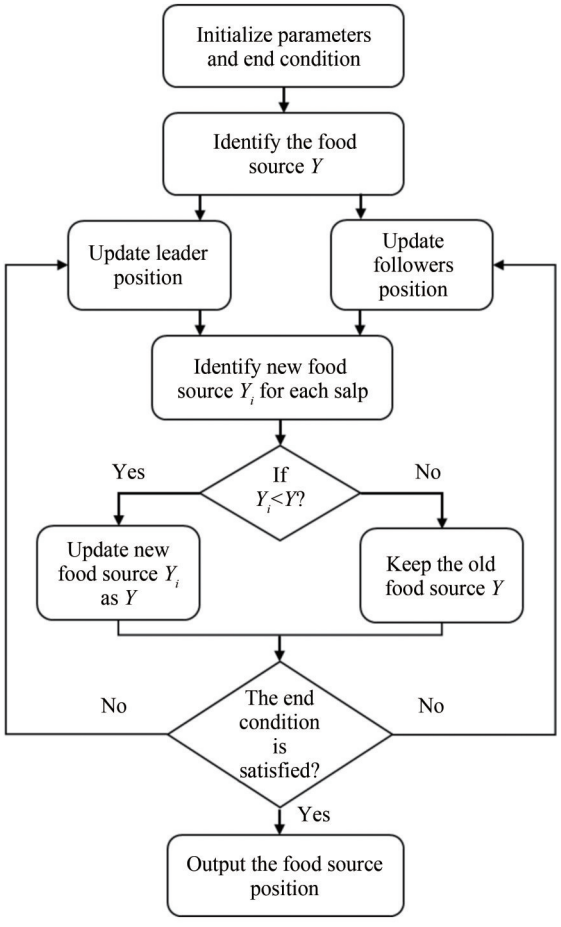

Figure 3 Flowchart for salp swarm optimization

3.3 Stability analysis

The path tracking control problem of an AUV in Equation (8) with assumptions (1)–(2) is considered. The control action is seletced as super twisting algorithm based SOSMC along with the adaptive PI law, then the path-tracking error vector asymptotically converges to zero.

Proof: The Lyapunov function candidate is as follows:

$$\boldsymbol{V} = \frac{1}{2}\left[\boldsymbol{\sigma}^{\mathrm{T}}\boldsymbol{\sigma} + \tilde{\boldsymbol{L}}^{\mathrm{T}}\boldsymbol{G}\tilde{\boldsymbol{L}}\right] \tag{32}$$

where, $\boldsymbol{G} \in \boldsymbol{R}^3$ is a diagonal positive definite constant matrix, and $\tilde{\boldsymbol{L}}$ is the estimation error vector of the lumped perturbation and is defined as follows:

$$\tilde{\boldsymbol{L}} = \boldsymbol{L}_{\text{est}} - \boldsymbol{L} \tag{33}$$

In above Equation (33), $\boldsymbol{L}_{\text{est}}$ and $\boldsymbol{L}$ are the estimated perturbation and the unknown actual perturbation vectors, respectively. The derivative of Lyapunov function is given as follows:

$$\dot{V} = \boldsymbol{\sigma}^{\mathrm{T}}\dot{\boldsymbol{\sigma}} + \tilde{\boldsymbol{L}}^{\mathrm{T}}\boldsymbol{G}\dot{\tilde{\boldsymbol{L}}}$$

$$\dot{V} = \boldsymbol{\sigma}^{\mathrm{T}}(2\Lambda\dot{e}_{\mathrm{c}} + \Lambda^2 e_{\mathrm{c}} + \ddot{e}_{\mathrm{c}}) + \tilde{\boldsymbol{L}}^{\mathrm{T}}\boldsymbol{G}\dot{\tilde{\boldsymbol{L}}}$$

$$\dot{V} = \boldsymbol{\sigma}^{\mathrm{T}}(2\Lambda\dot{e}_{\mathrm{c}} + \Lambda^2 e_{\mathrm{c}}) + \boldsymbol{\sigma}^{\mathrm{T}}\left(\ddot{\eta}_{\mathrm{c}} - \frac{1}{M(\eta)}(\tau_{\eta} - C(v) - D(v) - g(\eta))\right) +$$

$$\tilde{\boldsymbol{L}}^{\mathrm{T}}\boldsymbol{G}\dot{\tilde{\boldsymbol{L}}} = -\boldsymbol{\sigma}^{\mathrm{T}}KM^{-1}(\eta)(\tau_{\text{ad}} + \tau_{\text{STA}}) + \boldsymbol{\sigma}^{\mathrm{T}}\boldsymbol{L} + \tilde{\boldsymbol{L}}^{\mathrm{T}}\boldsymbol{G}\dot{\boldsymbol{L}}_{\text{est}} -$$

$$-\boldsymbol{\sigma}^{\mathrm{T}}K\left\{f_i(G_s\sigma) + f_i(G_{\text{is}}\int\sigma\mathrm{d}t)\right\} + \boldsymbol{\sigma}^{\mathrm{T}}\boldsymbol{L} + \tilde{\boldsymbol{L}}^{\mathrm{T}}\boldsymbol{G}\dot{\boldsymbol{L}}_{\text{est}} -$$

$$\tilde{\boldsymbol{L}}^{\mathrm{T}}\boldsymbol{G}\dot{\boldsymbol{L}} = -\boldsymbol{\sigma}^{\mathrm{T}}K\left\{f_p(G_s\sigma) + f_i(G_{\text{is}}\int\sigma\mathrm{d}t)\right\} + \boldsymbol{\sigma}^{\mathrm{T}}\boldsymbol{L} +$$

$$\tilde{\boldsymbol{L}}^{\mathrm{T}}\boldsymbol{G}\dot{\boldsymbol{L}}_{\text{est}} - \tilde{\boldsymbol{L}}^{\mathrm{T}}\boldsymbol{G}\dot{\boldsymbol{L}} \leqslant -\left\|\boldsymbol{\sigma}^{\mathrm{T}}\right\|K\left\|f_p(\boldsymbol{G}_s\boldsymbol{\sigma})\right\| -$$

$$\left\|\boldsymbol{\sigma}^{\mathrm{T}}\right\|K\left\|f_i(G_{\text{is}}\int\sigma\mathrm{d}t)\right\| + \left\|\boldsymbol{\sigma}^{\mathrm{T}}\right\|\|\boldsymbol{L}\| + \left\|\tilde{\boldsymbol{L}}^{\mathrm{T}}\right\|\|f_i(\sigma)\| -$$

$$\left\|\tilde{\boldsymbol{L}}^{\mathrm{T}}\right\|\boldsymbol{G}\left\|\dot{\boldsymbol{L}}\right\| \leqslant -\|\boldsymbol{\sigma}\|K - \|\boldsymbol{\sigma}\|K + \|\boldsymbol{\sigma}\|\|\boldsymbol{L}\| + \left\|\tilde{\boldsymbol{L}}\right\|\|\boldsymbol{\sigma}\| -$$

$$\left\|\tilde{\boldsymbol{L}}^{\mathrm{T}}\right\|\boldsymbol{G}\left\|\dot{\boldsymbol{L}}\right\| \leqslant -\|\boldsymbol{\sigma}\|\left\{2K - \|\boldsymbol{L}\| - \left\|\tilde{\boldsymbol{L}}\right\|\right\} - \left\|\tilde{\boldsymbol{L}}^{\mathrm{T}}\right\|\boldsymbol{G}\left\|\dot{\boldsymbol{L}}\right\|$$

For proposed controller, $\left\|\tilde{\boldsymbol{L}}^{\mathrm{T}}\right\| \approx 0$

$$\dot{V} \leqslant -\|\sigma\|K_f \tag{34}$$

K_f can be selected such that the value of $\hat{K}_f$ remains negative (i.e.,$-\hat{K}_f = -\Gamma$, where $\Gamma > 0$). Thus, the reaching condition $\sigma\dot{\sigma} < 0$ is satisfied and σ approaches zero as $t \to \infty$.

Remark 2: Chattering free sliding mode control law is proposed for the path following control of an AUV, where a new adaptive term (Meysar and Notash, 2010; Jin and Yang, 2014; Amer et al., 2011) that eliminates the high frequency control action inherent in a conventional SMC is developed. Adaptive PI term removes the need for a prior knowledge of upper bounds of uncertainties in the dynamic vehicle parameters (Amer et al., 2011).

Remark 3: Super twisting algorithm-based disturbance compensation (Chalanga et al., 2016) and PI uncertainty estimator (Meysar and Notash, 2010) replace the discontinuous term of a conventional SMC with an estimation of the perturbations in an adaptive manner.

Remark 4: The proposed control law incorporates adaptive term, continuously compensating for the effect of unknown system dynamics caused by poorly approximated nonlinear hydrodynamics or sudden environmental loads. In addition, adaptive term does not require the parametrization of a regressor matrix and an unknown parameter vector (Amer et al., 2011).

Remark 5: Super twisting algorithm based SOSMC is designed to achieve finite time estimation of the oceanic disturbances and to generate a smooth and continuous steering command signal.

Remark 6: The proposed STA SOSMC algorithm performs precisely under the influence of fast acting disturbances such as ocean currents and tides and its simple design of path tracking response offers a smooth response in minimum reaching time.

4 Simulation results

To demonstrate the path tracking control performance of the proposed controller in the horizontal plane by regulating heading angle, numerical simulation was conducted through the INFANTE AUV model using the MATLAB/Simulink tool. A flat-fish type AUV with two back thrusters that are similar and symmetrically positioned with respect to the longitudinal axis was considered. Thus, the vehicle is an under actuated system because it lacks a lateral thruster. The general and differential operating modes of the thrusters provide a force along the vehicles longitudinal axis and a torque about its vertical axis, respectively. In this work, only the back thrusters were used to maneuver in the horizontal plane. For the experimental AUV employed in the simulation, Lapierre and Soetanto (2007) provided the vehicle's physical specifications and hydrodynamic coefficients. In this simulation, which was conducted in the AUV's horizontal plane, typical circular and nonlinear path tracking were examined. The AUV's desired states were assumed to be $x_{\mathrm{d}} = 80\cdot\sin(0.01t)$ and $y_{\mathrm{d}} = 50\cdot\sin(0.01t)$, respectively, and their initial states were specified as zero. The path tracking problem of circular and nonlinear tracks was used to illustrate the robustness of the proposed controller by accounting for ambiguous circumstances and unidentified disruptions. To generate the time-varying disturbances and uncertainty indicated in the works of Wang et al., (2023b), Wang and Er (2016), and Lakhekar et al., (2019) without losing generality, the following parameters are given for evaluating control performance, $\Delta F_u = 0.1(m_{11} + \Delta m_{11}) + \delta_{\mathrm{d}}\sin(0.01t)$, $\Delta F_v = 0.1(m_{22} + \Delta m_{22}) + \delta_{\mathrm{d}}\sin(0.01t)$ and $\Delta F_w = 0.1(m_{33} + \Delta m_{33}) + \delta_{\mathrm{d}}\sin(0.01t)$ for evaluating control performance. In addition, $\delta_{\mathrm{d}} = 0.070\,7\,\mathrm{rand}(1, \mathrm{length}(t))$ and $(\cdot)$ is the Gaussian random noise signal.

The simulation results in Figure 4 represent circular and nonlinear path-tracking response in presence of oceanic disturbances along with uncertain operating conditions. In addition, the system parameters simultaneously increased by 20% compared with the actual parameter. In the pres-

ence of external perturbation and time-varying uncertain situations, terminal SMC and the proposed SOSMC control methodology outperformed other common methods, such as PD and conventional SMC. In the early phase of the simulation results, PD offered a quick response along with overshoot, whereas SMC required more time to reach the desired path without oscillation. While, terminal SMC and the proposed SOSMC method took a short time to reach the desired circular path in oceanic environment.

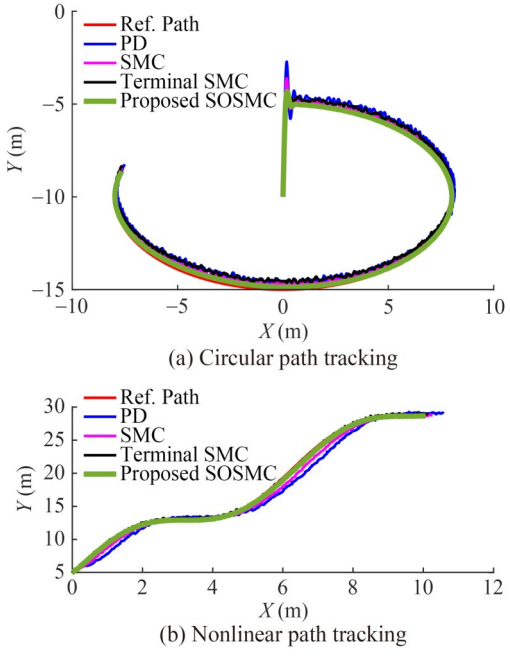

Figure 4 Path tracking in presence of adverse oceanic conditions

Compared with existing control strategies, the suggested planar control performed well in simulation results to reach and maintain the target path. Figure 5 displays the

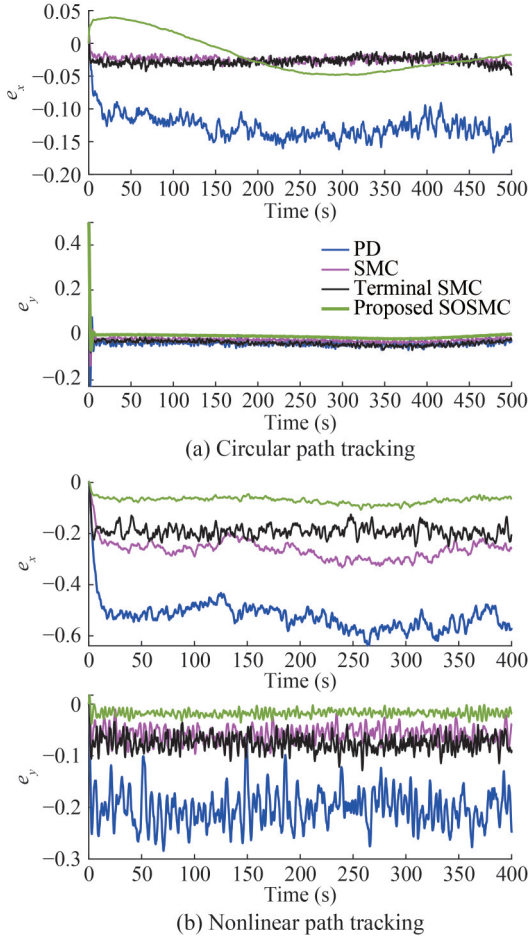

Figure 5 Errors under the effect of uncertainties and disturbances

path tracking errors in the *x*-*y* plane of the circular and nonlinear path, which was used in the quantitative analysis.

The simulation results in Figures 6 and 7 demonstrate response of the forward speed, heading angle, sway, and yaw velocity for circular and nonlinear path scenarios, in

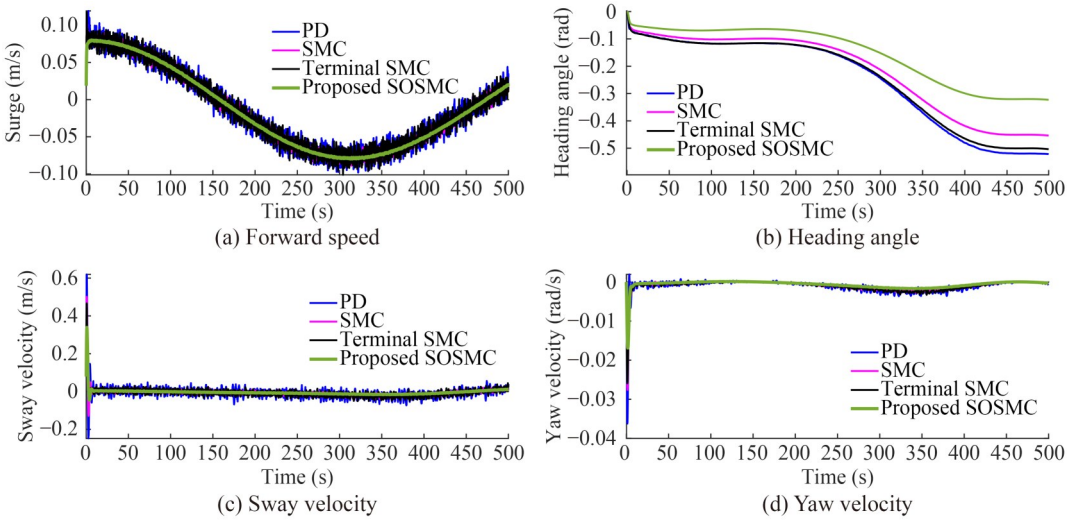

Figure 6 Circular path tracking

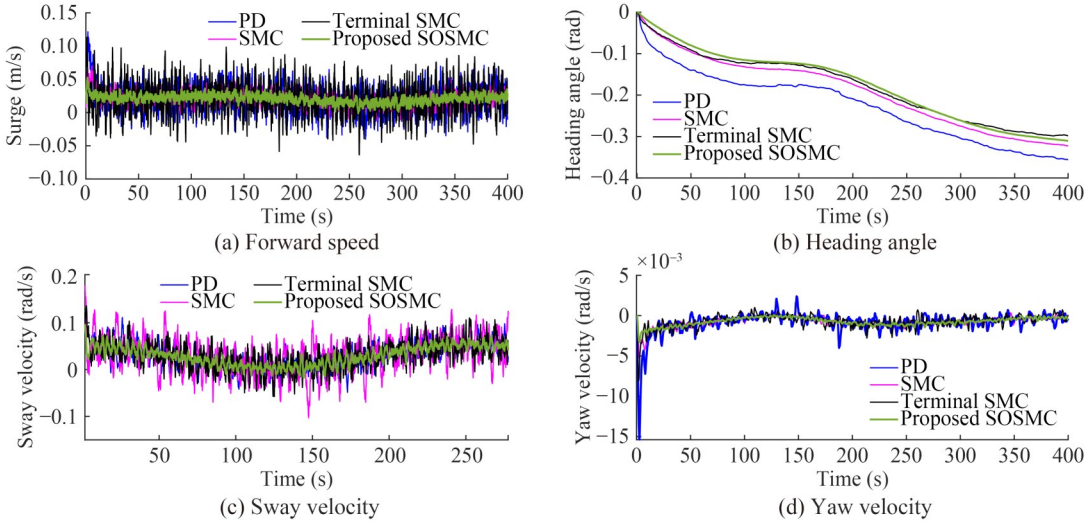

Figure 7 Nonlinear path tracking

presence of oceanic disturbances and noises. PD and conventional SMC exhibited a large settling time and were unable to attenuate the oceanic disturbances. In comparison, the proposed control strategy performed well in numerical simulation to reach and maintain the desired path.

To evaluate the tracking accuracy and efficacy of the proposed controller, anaysis was performed through quantitative methods based on performance measures such as Integral Square Error (ISE), Integral Absolute Error (IAE) and Root Mean Square Error (RMSE), as shown in Table 1. The proposed control scheme obtained the minimum tracking error compared with other controllers. Among all the controllers, the PD controller provided the maximum error in the circular and nonlinear path tracking control in adverse oceanic conditions.

Generating the symmetric bulb turn trajectory requires cosinusoidal reference signals. In the initial phase of simulation, The AUV experienceed an impulsive force due to ocean currents and waves. Thereby, some oscillation appeared in the path tracking response of PD and SMC, as depicted in Figure 8. The tracking performance was also evaluated under the influence of adverse oceanic conditions. However, proposed SOSMC needed minimum reaching time period with smooth response compared with other control techniques. Also able to cope with unexpected disturbances and parametric variations. The control performance was confirmed by quantitative analysis, as presented in Table 2.

5 Experimental validation

Experimental validation (Halil and Sümer, 2014) was conducted to confirm the efficacy of the control scheme further. The results from the experimental setup were obtained using National Instruments (NI) myRIO and Raspberry Pi 4 board setup. The setup verified the AUV performance in the presence of constant disturbances and uncertainties.

Figure 9 (a) shows that HIL simulation was designed to demonstrate real-time performance of the proposed control algorithm, as implemented through numerical simulation. Two hardware boards were used, one for AUV model deployment on Raspberry Pi4 and another for AUV controller on NI myRIO DAQ board setup for HIL validation,

Table 1 Quantitative analysis: Planar motion with 20% change in disturbances/uncertainty

Controller	Circular path tracking (m)						Nonlinear path tracking (m)					
	ISE		IAE		RMSE		ISE		IAE		RMSE	
	x_e	y_e	x_e	y_e	x_e	y_e	x_e	y_e	x_e	y_e	x_e	y_e
PD	7.522 3	4.425 3	17.891 0	15.042	3.578 0	3.438 2	4.246 8	3.985 3	14.031	12.453 4	1.453 2	1.253 4
SMC	3.125 3	2.457 2	11.784 0	13.621	2.672 1	2.178 4	3.259 2	2.145 2	10.153	9.257 8	1.054 3	0.843 2
TSMC	2.725 0	2.022 3	10.426 0	11.555	1.951 1	1.976 1	2.167 1	1.912 9	7.281	8.013 2	0.920 1	0.688 2
SOSMC	2.576 2	1.415 3	9.057 2	9.041	1.657 0	1.345 2	1.458 3	1.598 2	5.842	6.157 8	0.510 3	0.457 2

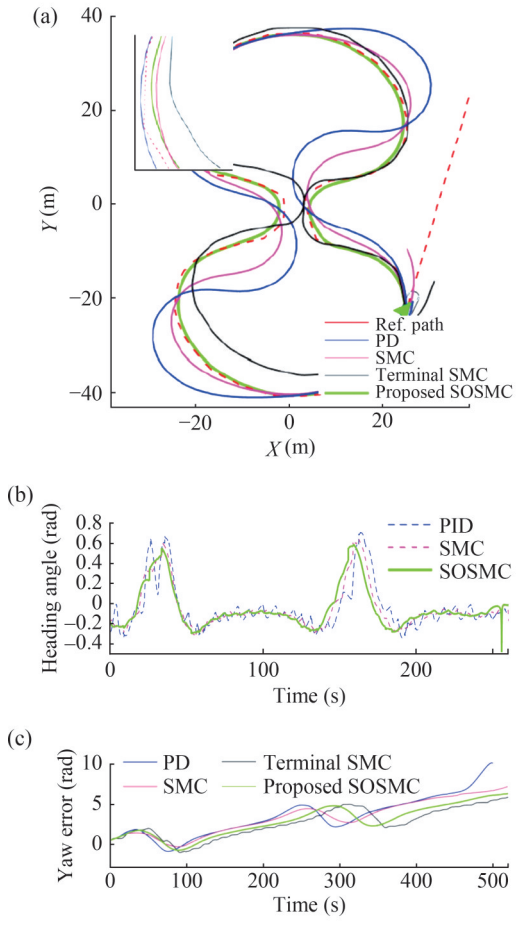

Figure 8 (a) Response of symmetric bulb turn path tracking; (b) Heading angle; (c) Yaw error

Table 2 Quantitative analysis: Bulb turn path following

Controller	ISE (m)		IAE (m)		RMSE (m)	
	x_e	y_e	x_e	y_e	x_e	y_e
PD	4.985 3	3.527 8	18.012 5	16.549 3	2.523 9	1.952 4
SMC	3.524 9	2.496 5	12.114 5	9.625 4	0.957 8	0.810 5
TSMC	3.185 1	2.221 3	8.995 1	8.257 5	0.882 1	0.622 5
SOSMC	1.583 4	0.925 7	2.953 7	3.827 9	0.698 5	0.525 4

as shown in Figure 9 (a). The NI myRIO board has an integrated Xilinx Zynq-7010 system-on-a-chip (SoC) technology, dual-core ARM® Cortex™-A9 processor, FPGA with 28 000 programmable logic cells, 10 analog inputs, 6 analog outputs, audio I/O channels, and up to 40 lines of digital input/output (DIO), including onboard Wi-Fi, a three-axis accelerometer. Raspberry Pi4 uses a Quad-core ARM Cortex-A72 at 1.5 GHz, 32 kB of data L1 cache and 48 kB of instruction L1 cache, and 1 MB of shared L2 cache. The real time proposed control algorithm designed through Simulink® models was compiled to C-code and deployed in the NI board. The onboard processor transmitted the command signals to Raspberry Pi 4 module, where an AUV model is deployed for path following applications in HIL testing.

A twisted path scenario was considered in experimental validation in presence of constant disturbances and parametric variations. In this complicated scenario, various waypoints were joined through a continuous desired path with wide turning. The experimental results in Figure 9 (b) indicate desired tracking performance of proposed SOSMC in nonlinear twisted path scenario, with minimum deviation at each turning point and requiring less settling time.

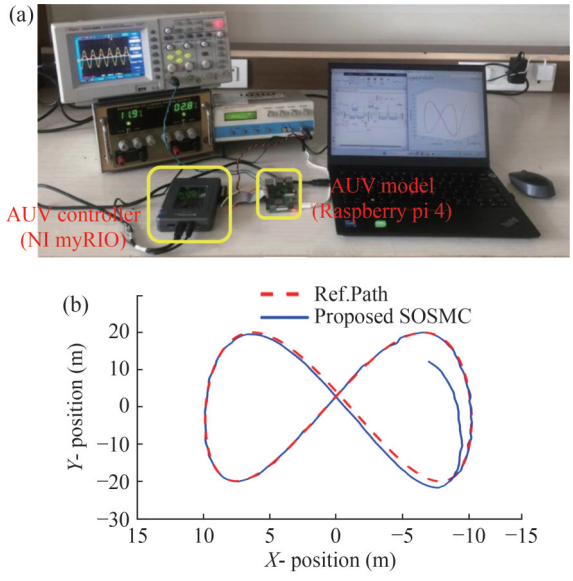

Figure 9 (a) A real time implementation of path following control of AUV model via hardware in loop simulation; (b) Response of path following HIL simulation

6 Conclusions

In this paper, a robust optimal super twisting SOSMC with uncertainty estimator based planar motion controller is designed for AUV path tracking in horizontal plane by precisely regulating heading angle. The proposed control technique takes advantage of second order sliding mode, uncertainty estimator, and super twisting method as a disturbance observer with SSW optimization, while the weaknesses attributed to these techniques are overcome by one another. The planar tracking control performance is evaluated under the influence of parametric uncertainties and oceanic disturbances for smooth turning behavior. Starting from initial conditions of the AUV states, the output positional variables asymptotically track desired circular path with a quick and robust response. Based on SSWO approach, hitting gain and sliding surface slope are adjusted through their appropriate optimal values. It is robust against unfavorable oceanic conditions with the help of STA and

adaptive control term as uncertainty estimator. Therefore, overall smooth tracking performance, quick hitting time and minimum chattering are achieved. The proposed technique is verified by demonstrative simulation results and experimental validation. The planar tracking control performance is quantified through performance indices and also analyzed through error convergence.

Acknowledgement The work is supported by the Center of Intelligent Mobility (CIM), KLE Technological University, Hubli, Karnataka and collaborated with the Department of Instrumentation and Control, COEP Technological University, Pune, Maharashtra. The authors would like to express their sincere gratitude to the Editor-in-Chief and anonymous reviewers whose constructive comments have helped us to significantly improve both the technical quality and presentation of this manuscript.

The authors are deeply grateful to the Head of the Department of Instrumentation and Control Engineering, COEP Technological University, Pune, M. S., for utilizing the laboratory to carry out research work.

Competing interest The authors have no competing interests to declare that are relevant to the content of this article.

References

Amer AF, Sallam EA, Elawady WM (2011) Adaptive fuzzy sliding mode control using supervisory fuzzy control for 3 DOF planar robot manipulators, Applied Soft Computing 11(8): 4943-4953. https://doi.org/10.1016/j.asoc.2011.06.005

Antonelli G, Chiaverini S, Sarkar N, West M (2001) Adaptive control of an autonomous underwater vehicle: experimental results on ODIN. IEEE Transactions on Control Systems Technology 9(5): 756-765. http://doi.org/10.1109/87.944470

Chalanga A, Kamal S, Fridman LM, Bandyopadhyay B, Moreno JA (2016) Implementation of super-twisting control: Super-twisting and higher order sliding-mode observer-based approaches. IEEE Trans Industr Electron 63(6): 3677-3685

Cheng Z, Wang J (2020) A new combined model based on multiobjective salp swarm optimization for wind speed forecasting, Applied Soft Computing 92(3): 106-120.https://doi.org/10.1016/j.asoc.2020.106294

DeBitetto PA (1995) Fuzzy logic for depth control of unmanned undersea vehicles, IEEE Journal of Oceanic Engineering 20(3): 242-248. DOI: 10.1109/48.393079

Elmokadem T, Zribi M, Youcef-Toumi K (2016) Trajectory tracking sliding mode control of underactuated AUVs, Nonlinear Dynamics 84(2): 1079-1091. https://doi.org/10.1007/s11071-015-2551-x

Feng Z, Allen R (2004) Reduced order H∞ control of an autonomous underwater vehicle, Control Engineering Practice 13(4): 1511-1520. https://doi.org/10.1016/S1474-6670(17)36668-5

Fossen TI(1994) Guidance and Control of Ocean Vehicles. Hoboken, NJ: John Wiley and Sons, 448-451

Geranmehr B, Nekoo SR (2015) Nonlinear suboptimal control of fully coupled non-affine six-DOF autonomous underwater vehicle using the state-dependent Riccati equation, Ocean Engineering 96(1): 248-257. https://doi.org/10.1016/j.oceaneng.2014.12.032

Goheen KR, Jefferys ER (1990) Multivariable self-turning autopilots for autonomous underwater vehicles, IEEE Journal of Oceanic Engineering 15(3): 144-151. DOI: 10.1109/48.107142

Guo J, Chiu FC, Huang CC (2003) Design of a sliding mode fuzzy controller for guidance and control of an autonomous underwater vehicle, Ocean Engineering 30(16): 2137-2155. https://doi.org/10.1016/S0029-8018(03)00048-9

Halil A, Sümer LG (2014), Robust control of variable speed autonomous underwater vehicle, Advanced Robotics, Taylor & Francis, 28: 601-611, http://doi.org/10.1080/01691864.2013.879370

Innocenti M, Campa G (1999) Robust control of underwater vehicles: sliding mode Vs LMI synthesis, Proceeding of the 1999 American Control Conference 5(1): 3422-3426. http://doi.org/10.1109/ACC.1999.782400

Jalving B (1994) The NDRE-AUV flight control system. IEEE Journal of Oceanic Engineering 19(4): 497-501. http://doi.org/10.1109/48.338385

Jin Li, Yang L (2014) Adaptive PI-based sliding mode control for nanopositioning of piezoelectric actuators. Mathematical Problems in Engineering 2014: Article ID 357864. https://doi.org/10.1155/2014/357864

Kim MM, Joe H, Kim J, Yu SC (2015) Integral sliding mode controller for precise manoeuvring of autonomous underwater vehicle in the presence of unknown environmental disturbances, International Journal of Control 26(2): 1-11. https://doi.org/10.1080/00207179.2015.1031182

Kumar S, Soni SK, Sachan A, Kamal S, Bandyopadhyay B (2022) Adaptive super-twisting guidance law: An event-triggered approach. 2022 16th International Workshop on Variable Structure Systems (VSS), Rio de Janeiro, Brazil 190-195, https://doi.org/10.1109/VSS57184.2022.9901685

Lakhekar GV, Roy RG (2014) Heading control of an underwater vehicle using dynamic fuzzy sliding mode controller. 2014 International Conference on Circuits, Power and Computing Technologies [ICCPCT-2014], Piscataway:IEEE 2014: 1448-1454. https://doi.org/10.1109/ICCPCT.2014.7054969

Lakhekar G V, Saundarmal VD (2013) Robust self tuning of fuzzy sliding mode control, International Conference on Computing, Communications and Networking Technologies (ICCCNT), Tiruchengode, India 1-7. https://doi.org/10.1109/ICCCNT.2013.6726610

Lakhekar GV, Waghmare LM (2023) Robust self-organising fuzzy sliding mode-based path-following control for autonomous underwater vehicles. Journal of Marine Engineering & Technology 22(3):131-152. https://doi.org/10.1080/20464177.2022.2120448

Lakhekar GV, Waghmare LM (2014) Dynamic fuzzy sliding mode control of underwater vehicles. Springer Book Publication Book Chapter: Advances and Applications in Sliding Mode Control systems (Studies in Computational Intelligence) 576 XIV, 628, 280 illus

Lakhekar GV, Waghmare LM, Roy RG (2019) Disturbance observer-based fuzzy adapted S-surface controller for spatial trajectory tracking of autonomous underwater vehicle. IEEE Transactions on Intelligent Vehicles, 4(4): 622-636. https://doi.org/10.1109/TIV.2019.2938082

Lakhekar GV, Waghmare LM, Jadhav PG, Roy RG (2020) Robust diving motion control of an autonomous underwater vehicle using adaptive neuro-fuzzy sliding mode technique. IEEE Access 8: 109891-109904. https://doi.org/10.1109/ACCESS.2020.3001631

Lakhekar GV, Waghmare LM (2018) Adaptive fuzzy exponential terminal sliding mode controller design for nonlinear trajectory tracking control of autonomous underwater vehicle. Int. J. Dynam. Control 6: 1690-1705. https://doi.org/10.1007/s40435-017-0387-6

Lapierre L, Soetanto D (2007) Nonlinear path-following control of

an AUV. Ocean Engineering, 634(11): 1734-1744. https://doi.org/10.1016/j.oceaneng.2006.10.019

Meysar Z, Notash L (2010) Adaptive sliding mode control with uncertainty estimator for robot manipulators. Mechanism and Machine Theory 45(1): 80-90. https://doi.org/10.1016/j.mechmachtheory.2009.08.003

Moura A, Rijo R, Silva P, Crespo S (2010) A multi-objective genetic algorithm applied to autonomous underwater vehicles for sewage outfall plume dispersion observations. Applied Soft Computing 10(4): 1119-1126. https://doi.org/10.1016/j.asoc.2010.05.009

Naeem W, Sutton R, Ahmad SM (2003) LQG/ LTR control of an autonomous underwater vehicle using a hybrid guidance law. Ocean Engineering 36(4): 31-36. https://doi.org/10.1016/S1474-6670(17)36653-3

Naik MS, Singh SN (2007) State-dependent Riccati equation-based robust dive plane control of AUV with control constraints, Ocean Engineering 34(11): 1711-1723. https://doi.org/10.1016/j.oceaneng.2006.10.014

Nakamura Y, Savant S (1992) Nonlinear tracking control of autonomous underwater vehicles. IEEE International Conference on Robotics and Automation, 3: A4-A9. https://doi.org/10.1109/ROBOT.1992.220005

Pisano A, Usai E (2004) Output-feedback control of an underwater vehicle prototype by higher-order sliding modes. Automatica 40(9): 1525-1531. https://doi.org/10.1016/j.automatica.2004.03.016

Rout R, Subudhi B (2016) A backstepping approach for the formation control of multiple autonomous underwater vehicles using a leaderfollower strategy. Journal of Marine Engineering and Technology 15(1): 38-46. https://doi.org/10.1080/20464177.2016.1173268

Sadala SP, Patre BM (2020) Super-twisting control using higher order disturbance observer for control of SISO and MIMO coupled systems, ISA Transactions 106: 303-317. https://doi.org/10.1016/j.isatra.2020.06.016

Sahu BK, Subudhi B (2014) Adaptive tracking control of an autonomous underwater vehicle, International Journal of Automation and Computing 11(3): 299-307. https://doi.org/10.1007/s11633-014-0792-7

Shet RM, Lakhekar GV, Iyer NC (2023) Design of quasi fuzzy sliding mode based maneuvering of autonomous vehicle. Int. J. Dynam. Control. https://doi.org/10.1007/s40435-023-01308-0

Silvestre C, Pascoal A, Kaminer I (2002) On the design of gain scheduled trajectory tracking controllers. International Journal of Robust and Nonlinear Control 12: 797-839. https://doi.org/10.1002/rnc.705

Wang N, Er MJ (2016) Direct Adaptive Fuzzy Tracking Control of Marine Vehicles With Fully Unknown Parametric Dynamics and Uncertainties. IEEE Transactions on Control Systems Technology, 24(5): 1845-1852 https://doi.org/10.1109/TCST.2015.2510587

Wang N, He H, Hou Y, Han B (2023a) Model-free visual servo swarming of manned-unmanned surface vehicles with visibility maintenance and collision avoidance. IEEE Transactions on Intelligent Transportation Systems 25(1):697-709. https://doi.org/10.1109/TITS.2023.3310430

Wang N, Liu Y, Liu J, Jia W, Zhang C (2023b) Reinforcement learning swarm of self-organizing unmanned surface vehicles with unavailable dynamics. Ocean Engineering 289(2): 116313. https://doi.org/10.1016/j.oceaneng.2023.116313

Yoerger D, Slotine J (1985) Robust trajectory control of underwater vehicles, IEEE Journal of Oceanic Engineering 10(4): 462-470. https://doi.org/10.1109/UUST.1985.1158537

Yuh J (1990) A neural net controller for underwater robotic vehicles, IEEE Journal of Oceanic Engineering 15(3): 161-166. https://doi.org/10.1109/48.107144